Computational Materials Science 51 (2012) 353–359

Contents lists available at SciVerse ScienceDirect

Computational Materials Science

journal homepage: www.elsevier.com/locate/commatsci

Explicit cross-link relations between effective elastic modulus and thermal conductivity for fiber composites

Fei Song [a,1], Haifeng Zhao [b,*], Gengkai Hu [a,*]

[a] School of Aerospace Engineering, Beijing Institute of Technology, Beijing 100081, People's Republic of China
[b] Department of Aerospace Engineering and Engineering Mechanics, The University of Texas at Austin, Austin, TX 78712, USA

ARTICLE INFO

Article history:
Received 20 April 2011
Received in revised form 5 July 2011
Accepted 14 July 2011

Keywords:
Fiber composite
Fiber orientation
Cross-property relation
Numerical method
Analytical method

ABSTRACT

Explicit cross-link relations between effective elastic modulus and thermal conductivity for composites with different fiber orientation are derived with help of Mori–Tanaka micromechanical method. Numerical cross-link relations are also established by digital-image-based finite element method, and they compare favorably with the analytical cross-link relations especially for the composite with aligned fibers and planar randomly oriented fibers. Both analytical and numerical cross-link relations agree well with the experimental results available in the literature. For the composite with space randomly oriented fibers, the numerically obtained cross-link relations are insensitive to the fiber's shape, and the analytical cross-link relations are weakly dependent on fiber's shape. In sum, the sensitivity of cross-link relations to the fiber's shape depends on the extent of anisotropic behavior of fiber composites. Such cross-link relations can be potentially applied for predicting the difficult-to-measure elastic modulus from the measured thermal conductivities.

1. Introduction

The overall elastic modulus, electrical/thermal/magnetic conductivity, dielectric coefficient and thermal expansion coefficient, are typically functions of the same microstructural parameters for a specified composite material. By eliminating all or partially these parameters, we can obtain the cross-link relations between two different classes of overall properties, e.g. elastic modulus and thermal conductivity. These cross-link relations are useful to determine one class of property in term of the others, especially when one class of property is difficult to measure. Bristow [1] was probably the first to establish approximately such cross-link relation between elastic modulus and conductivity for a solid containing low density, randomly oriented microcracks. The exact correlation between the effective bulk modulus and the thermal expansion coefficient for a fiber-reinforced composite was subsequently derived by Levin [2]. Based on non-interaction approximation, Lu et al. [3] established the correlations between the effective modulus and thermal conductivity of thermal barrier coatings (TBCs) for a variety of anisotropic pore morphologies, a similar work can be found in Sevostianov and Kachanov [4] for plasma sprayed ceramic coatings. Kachanov et al. [5] and Sevostianov and Kachanov [6] derived, also in the framework of non-interaction approximation, explicit correlations between the effective modulus and electrical conductivity of two-phase composites and porous materials with anisotropic microstructures. Based on the analytical micromechanical method and numerical method, Zhao et al. [7,8] examined the cross-link relation between elastic modulus and conductivity for a general planar composite, the influence of microstructure on such cross-link relation was studied in detail. It was found that the correlation relations are insensitive to the microstructure for moderate phase contrast. A very comprehensive review on the cross-link relation and sensitivity to inhomogeneities was presented by Sevostianov and Kachanov [9]. Recently, Sevostianov and Shrestha [10] also developed a cross-link relation between electrical conductivity and fluid permeability of a porous material with randomly distributed interconnected phases. Experimental investigation of the cross-property link between the effective modulus and thermal conductivity was addressed by Sevostianov et al. [11] for close-celled aluminum foams and by Sevostianov and Kachanov [12] for short fiber-reinforced thermoplastics. The elastic modulus and thermal conductivity of composites with aligned fiber and planar randomly oriented fiber were measured by Rousion et al. [13].

The focus of this paper is on two-phase composites with different fiber orientations, both numerical and analytical methods have been utilized to obtain the cross-property relations. The influence of microstructures and reinforced phase property on the cross-links is examined. The paper is arranged as follows: explicit

* Corresponding authors. Present address: GE Global Research Center, Niskayuna, NY 12309, USA (H.F. Zhao). Tel./fax: +86 010 68914538.
E-mail addresses: hfzhao@ices.utexas.edu (H.F. Zhao), hugeng@bit.edu.cn (G.K. Hu).
[1] Present address: Department of Applied Science, University of Arkansas at Little Rock, Little Rock, AR 72204, USA.

0927-0256/$ - see front matter © 2011 Elsevier B.V. All rights reserved.
doi:10.1016/j.commatsci.2011.07.031

Nomenclature

c	volume fraction
E	Young's modulus
K	bulk modulus ($K = E/3/(1-2\nu)$)
Greek symbols	
ρ	aspect ratio of the ellipsoid
ν	Poisson's ratio
μ	shear modulus ($\mu = E/2/(1+\nu)$)
Bold symbols	
$\boldsymbol{L}$	stiffness tensor
$\boldsymbol{k}$	thermal conductivity tensor
Subscripts	
0	matrix
1	fiber
c	composite
Decoration	
$\sim$	same quantity as in elasticity
–	effective quantity
Operation	
{}	orientational average
$\otimes$	tensor product

cross-link relations are derived analytically by Mori–Tanaka's micromechanical method [14] in Section 2; In Section 3, numerical cross-property relations are established by finite element method, and they have been compared with the analytical, and experimental results available in the literature.

2. Analytical cross-link relations

In the following, Mori–Tanaka's mean field theory [14] is utilized to evaluate the effective modulus and thermal conductivity for composite materials. Since this method is widely used to predict the effective property for composite materials, here only final results are provided. For a two-phase composite, the effective stiffness and thermal conductivity of the composite are given respectively by [15]

$$\boldsymbol{L}_c = \boldsymbol{L}_0 + c_1(\boldsymbol{L}_1 - \boldsymbol{L}_0)\left[c_0\{\boldsymbol{T}_1\}^{-1} + c_1\boldsymbol{I}\right]^{-1} \tag{1a}$$

$$\boldsymbol{k}_c = \boldsymbol{k}_0 + c_1(\boldsymbol{k}_1 - \boldsymbol{k}_0)\left[c_0\{\widetilde{\boldsymbol{T}}_1\}^{-1} + c_1\widetilde{\boldsymbol{I}}\right]^{-1} \tag{1b}$$

where $\boldsymbol{L}, \boldsymbol{k}$ denote the stiffness tensor and thermal conductivity tensor, respectively. The indices 0, 1 and c refer, separately, to the matrix, the fiber and the composite. c_0 and c_1 are respectively the volume fractions of the matrix and fiber. The quantity with an overbar means the same quantity as in elasticity, however it is a second order tensor. {} means orientational average operation, defined by:

for planar randomly oriented fibers

$$\{\bullet\} = \frac{1}{\pi}\int_0^{\pi} \bullet\, d\vartheta \tag{2}$$

and for space randomly oriented fibers

$$\{\bullet\} = \frac{1}{4\pi}\int_0^{\pi}\int_0^{2\pi} \bullet \sin\vartheta\, d\varphi\, d\vartheta \tag{3}$$

where $\boldsymbol{T}_1 = [\boldsymbol{I} + \boldsymbol{P}_1(\boldsymbol{L}_1 - \boldsymbol{L}_0)]^{-1}$, $\widetilde{\boldsymbol{T}}_1 = \left[\widetilde{\boldsymbol{I}} + \widetilde{\boldsymbol{P}}_1(\boldsymbol{k}_1 - \boldsymbol{k}_0)\right]^{-1}$, the tensors $\boldsymbol{P}_1, \widetilde{\boldsymbol{P}}_1$ for a general ellipsoidal fiber are given in the appendices. Eqs. (1a,b) can be further recast as

$$[(\boldsymbol{L}_c - \boldsymbol{L}_0)^{-1}(\boldsymbol{L}_1 - \boldsymbol{L}_0) - \boldsymbol{I}]\{\boldsymbol{T}_1\} = \frac{c_0}{c_1}\boldsymbol{I} \tag{4a}$$

$$[(\boldsymbol{k}_c - \boldsymbol{k}_0)^{-1}(\boldsymbol{k}_1 - \boldsymbol{k}_0) - \widetilde{\boldsymbol{I}}]\{\widetilde{\boldsymbol{T}}_1\} = \frac{c_0}{c_1}\widetilde{\boldsymbol{I}} \tag{4b}$$

In order to eliminate the volume fraction of the fiber, we multiply both side of Eq. (4a) a second order tensor $\widetilde{\boldsymbol{I}}$. There are different ways to reduce a fourth order unit tensor to a second one. For a fourth order tensor $I_{ijkl} = \frac{1}{2}(\delta_{ik}\delta_{jl} + \delta_{il}\delta_{jk})$, it is easy to show that $I_{ijkl}\delta_{kl} = \delta_{ij} = \widetilde{I}_{ij}$, $I_{ijkl}\delta_{ik} = 2\delta_{jl} = 2\widetilde{I}_{jl}$, $I_{ijkl}\delta_{ij} = \delta_{kl} = \widetilde{I}_{kl}$. We note these operations by $\boldsymbol{I} : \widetilde{\boldsymbol{I}} = \widetilde{\boldsymbol{I}}$, $\boldsymbol{I} \circ \widetilde{\boldsymbol{I}} = 2\widetilde{\boldsymbol{I}}$, $\widetilde{\boldsymbol{I}} : \boldsymbol{I} = \widetilde{\boldsymbol{I}}$, respectively. With these different rules in mind, we can eliminate the volume fraction of fiber from Eqs. (4a,b), leading to

$$[(\boldsymbol{L}_c - \boldsymbol{L}_0)^{-1}(\boldsymbol{L}_1 - \boldsymbol{L}_0) - \boldsymbol{I}]\{\boldsymbol{T}_1\} : \widetilde{\boldsymbol{I}} = [(\boldsymbol{k}_c - \boldsymbol{k}_0)^{-1}(\boldsymbol{k}_1 - \boldsymbol{k}_0) - \widetilde{\boldsymbol{I}}]\{\widetilde{\boldsymbol{T}}_1\} \tag{5a}$$

$$[(\boldsymbol{L}_c - \boldsymbol{L}_0)^{-1}(\boldsymbol{L}_1 - \boldsymbol{L}_0) - \boldsymbol{I}]\{\boldsymbol{T}_1\} \circ \widetilde{\boldsymbol{I}} = 2[(\boldsymbol{k}_c - \boldsymbol{k}_0)^{-1}(\boldsymbol{k}_1 - \boldsymbol{k}_0) - \widetilde{\boldsymbol{I}}]\{\widetilde{\boldsymbol{T}}_1\} \tag{5b}$$

$$\widetilde{\boldsymbol{I}} : [(\boldsymbol{L}_c - \boldsymbol{L}_0)^{-1}(\boldsymbol{L}_1 - \boldsymbol{L}_0) - \boldsymbol{I}]\{\boldsymbol{T}_1\} = [(\boldsymbol{k}_c - \boldsymbol{k}_0)^{-1}(\boldsymbol{k}_1 - \boldsymbol{k}_0) - \widetilde{\boldsymbol{I}}]\{\widetilde{\boldsymbol{T}}_1\} \tag{5c}$$

Eqs. (5a-c) form the general explicit cross-link relations between the effective stiffness tensor and thermal conductivity, derived from the approximate Mori–Tanaka's method. These relations are independent of the volume fraction of fiber. In the following, some specific applications of Eqs. (5a–c) will be illustrated.

2.1. Particulate composites

In this case, the tensors appeared in Eq. (5) are all isotropic, any isotropic fourth order tensor and its inverse can be written in the following form:

$$H_{ijkl} = K_H\delta_{ij}\delta_{kl} + \mu_H\left(\delta_{il}\delta_{jk} + \delta_{ik}\delta_{jl} - \frac{2}{3}\delta_{ij}\delta_{kl}\right) \tag{6a}$$

$$H^{-1}_{ijkl} = \frac{1}{K_H}\delta_{ij}\delta_{kl} + \frac{1}{\mu_H}\left(\delta_{il}\delta_{jk} + \delta_{ik}\delta_{jl} - \frac{2}{3}\delta_{ij}\delta_{kl}\right) \tag{6b}$$

An isotropic fourth order tensor and its inverse can be written in a compact form as $\boldsymbol{H} = (3K_H, 2\mu_H)$, $\boldsymbol{H}^{-1} = \left(\frac{1}{3K_H}, \frac{1}{2\mu_H}\right)$. It can be easily shown that $\boldsymbol{H} : \widetilde{\boldsymbol{I}} = 3K_H\widetilde{\boldsymbol{I}}$, and $\boldsymbol{H} \circ \widetilde{\boldsymbol{I}} = \left(K_H + \frac{10}{3}\mu_H\right)\widetilde{\boldsymbol{I}}$. Now we write the stiffness tensor and the tensor $\boldsymbol{P}_1$ in a compact form as: $\boldsymbol{L}_c = (3K_c, 2\mu_c)$, $\boldsymbol{L}_1 = (3K_1, 2\mu_1)$, $\boldsymbol{L}_0 = (3K_0, 2\mu_0)$ and $\boldsymbol{P}_1 = (3K_P, 2\mu_P)$, where for a spherical inclusion $K_p = \frac{1}{3(4\mu_0+3K_0)}$, $\mu_p = \frac{3(2\mu_0+K_0)}{10\mu_0(4\mu_0+3K_0)}$.

It can be shown that the following relations hold

$$[(\boldsymbol{L}_c - \boldsymbol{L}_0)^{-1}(\boldsymbol{L}_1 - \boldsymbol{L}_0) - \boldsymbol{I}]\boldsymbol{T}_1 = \left(\left[\frac{(K_1 - K_0)}{(K_c - K_0)} - 1\right]\frac{1}{[1 + 9K_p(K_1 - K_0)]}, \left[\frac{(\mu_1 - \mu_0)}{(\mu_c - \mu_0)} - 1\right]\frac{1}{[1 + 4\mu_p(\mu_1 - \mu_0)]}\right)$$

$$[(\boldsymbol{k}_c-\boldsymbol{k}_0)^{-1}(\boldsymbol{k}_1-\boldsymbol{k}_0)-\widetilde{\boldsymbol{I}}]\widetilde{\boldsymbol{T}}_1=\left[\frac{k_1-k_0}{k_c-k_0}-1\right]\frac{3k_0}{k_1+2k_0}\widetilde{\boldsymbol{I}}$$

Eqs. (5a–c) give the explicit correlations between the bulk modulus and the effective thermal conductivity of the composite.

$$\left[\frac{(\overline{K}_1-1)}{(\overline{K}_c-1)}-1\right]+\frac{3[1+9\overline{K}_p(\overline{K}_1-1)]}{\bar{k}_1+2}\left[\frac{(\bar{k}_1-1)}{(\bar{k}_c-1)}-1\right] \tag{7a}$$

$$\left[\frac{(\overline{K}_1-1)}{(\overline{K}_c-1)}-1\right]+\frac{5[1+9\overline{K}_p(\overline{K}_1-1)]}{1+4\bar{\mu}_p(\bar{\mu}_1-1)}\left[\frac{(\bar{\mu}_1-1)}{(\bar{\mu}_c-1)}-1\right]=\frac{18[1+9\overline{K}_p(\overline{K}_1-1)]}{\overline{K}_1+2}\left[\frac{(\bar{k}_1-1)}{(\bar{k}_c-1)}-1\right] \tag{7b}$$

where $\overline{K}_1=K_1/K_0,\overline{K}_c=K_c/K_0,\bar{\mu}_1=\mu_1/\mu_0,\bar{\mu}_c=\mu_c/\mu_0$ and $\overline{\mu}_P=\mu_P\mu_0,\overline{K}_P=K_PK_0,\overline{K}_1=k_1/k_0$ and $\overline{K}_c=k_c/k_0$. They are non dimensional quantities.

Eqs. (7a,b) finally give the cross-link relation between the shear modulus and the thermal conductivity as

$$\left[\frac{(\bar{\mu}_1-1)}{(\bar{\mu}_c-1)}-1\right]=\frac{3[1+4\bar{\mu}_p(\bar{\mu}_1-1)]}{\overline{K}_1+2}\left[\frac{(\bar{k}_1-1)}{(\bar{k}_c-1)}-1\right] \tag{8}$$

So Eqs. (7a) and (8) form the basic explicit cross-link relations between the effective modulus and the thermal conductivity for a particulate composite, derived from Mori–Tanaka's method.

2.2. Composites with space randomly oriented fibers

In this situation, the composite as a whole is isotropic, and the tensor $\{\boldsymbol{T}_1\}$ is also isotropic, and noted by$\{\boldsymbol{T}_1\}=(3K_T,2\mu_T)$. For ellipsoidal fibers, we note the $\boldsymbol{P}_1$ tensor as $\boldsymbol{P}_1'$, in the local principle coordinate system attached with x_1' being the symmetrical axis of the ellipsoidal fiber. In this coordinate system, $\boldsymbol{P}_1'$ is written as $P_1'=(P_{2222}+P_{2233},P_{1122},P_{1122},P_{1111},2P_{2323},2P_{1212})$, the physical interpretations of these notation are provided by Hashin [16]. Let $\boldsymbol{I}+\boldsymbol{P}_1'(\boldsymbol{L}_1-\boldsymbol{L}_0)=(c,g,h,d,e,f)$, where

$$c=1+\frac{2}{3}(\mu_0-\mu_1)(2P_{1122}-P_{2222}-P_{2233})-3(K_0-K_1)\times(P_{1122}+P_{2222}+P_{2233}) \tag{9a}$$

$$g=\frac{2}{3}(\mu_0-\mu_1)(P_{1111}-P_{1122})-(K_0-K_1)(P_{1111}+2P_{1122}) \tag{9b}$$

$$h=-\left[\frac{4}{3}(\mu_0-\mu_1)+K_0-K_1\right]P_{1122}+\left[\frac{2}{3}(\mu_0-\mu_1)-K_0+K_1\right](P_{2222}+P_{2233}) \tag{9c}$$

$$d=1-\frac{4}{3}(\mu_0-\mu_1)(P_{1111}-P_{1122})-(K_0-K_1)(P_{1111}+2P_{1122}) \tag{9d}$$

$$e=1-4(\mu_0-\mu_1)P_{2323} \tag{9e}$$

$$f=1-4(\mu_0-\mu_1)P_{1212} \tag{9f}$$

We note the tensor $\boldsymbol{T}_1$ in the local coordinate system as $\boldsymbol{T}'=[\boldsymbol{I}+\boldsymbol{P}_1'(\boldsymbol{L}_1-\boldsymbol{L}_0)]^{-1}=\{2k_T,l_T,l_T',n_T,2m_T,2p_T\}$, where

$$2k_T=d/(cd-2gh),\quad l_T=-g/(cd-2gh),\quad l_T'=-h/(cd-2gh),\quad 2m_T=1/e,\quad 2p_T=1/f$$

The space orientational average of the tensor $\boldsymbol{T}'$ leads to

$$\{\boldsymbol{T}'\}=(3K_{3D},2\mu_{3D}) \tag{10}$$

where

$$K_{3D}=\frac{1}{9}(4k_T+2l_T+2l_T'+n_T),$$

$$\mu_{3D}=\frac{1}{15}[k_T-(l_T+l_T')+n_T+6(m_T+p_T)]$$

Finally, it can be shown that

$$[(\boldsymbol{L}_c-\boldsymbol{L}_0)^{-1}(\boldsymbol{L}_1-\boldsymbol{L}_0)-\boldsymbol{I}]\{\boldsymbol{T}_1'\}=\left(3K_{3D}\left[\frac{(K_1-K_0)}{(K_c-K_0)}-1\right],2\mu_{3D}\left[\frac{(\mu_1-\mu_0)}{(\mu_c-\mu_0)}-1\right]\right) \tag{11}$$

For the thermal conductivity of the same composite, in the local coordinate system, the non-zero components of the tensor $\widetilde{\boldsymbol{P}}_1'$ are $\widetilde{P}_{11},\widetilde{P}_{22}=\widetilde{P}_{33}$. The non-zero components of the tensor $\widetilde{\boldsymbol{T}}_1=\left[\widetilde{\boldsymbol{I}}+\widetilde{\boldsymbol{P}}_1(\boldsymbol{k}_1-\boldsymbol{k}_0)\right]^{-1}$ in the local coordinate are respectively $\widetilde{T}_{11}=\frac{1}{1+\widetilde{P}_{11}(k_1-k_0)},\widetilde{T}_{22}=\widetilde{T}_{33}=\frac{1}{1+\widetilde{P}_{22}(k_1-k_0)}$. The space orientational average of the tensor $\widetilde{T}_1$ is isotropic, it is noted as $\{\widetilde{\boldsymbol{T}}_1\}=k_{3D}\widetilde{\boldsymbol{I}}$, and $k_{3D}=1/3(\widetilde{T}_{11}+2\widetilde{T}_{22})$, finally we can show that$[(\boldsymbol{k}_c-\boldsymbol{k}_0)^{-1}(\boldsymbol{k}_1-\boldsymbol{k}_0)-\widetilde{\boldsymbol{I}}]\{\widetilde{\boldsymbol{T}}_1\}=k_{3D}\left[\frac{k_1-k_0}{k_c-k_0}-1\right]\widetilde{\boldsymbol{I}}$. The cross-link relation between the effective modulus and thermal conductivity of the composite with space randomly oriented fibers can be derived by following the same method as the particulate composite, and this gives

$$\left[\frac{(\overline{K}_1-1)}{(\overline{K}_c-1)}-1\right]=\frac{k_{3D}}{3K_{3D}}\left[\frac{\overline{k}_1-1}{\overline{k}_c-1}-1\right] \tag{12a}$$

$$K_{3D}\left[\frac{(\overline{K}_1-1)}{(\overline{K}_c-1)}-1\right]+\frac{10\mu_{3D}}{3}\left[\frac{(\bar{\mu}_1-1)}{(\bar{\mu}_c-1)}-1\right]=k_{3D}\left[\frac{\overline{k}_1-1}{\overline{k}_c-1}-1\right] \tag{12b}$$

Eqs. (12a,b) together give finally

$$\left[\frac{(\bar{\mu}_1-1)}{(\bar{\mu}_c-1)}-1\right]=\frac{k_{3D}}{5\mu_{3D}}\left[\frac{\overline{k}_1-1}{\overline{k}_c-1}-1\right] \tag{13}$$

Eqs. (12a) and (13) provide the analytical cross-link relations between the effective modulus and thermal conductivity for isotropic composites with space randomly oriented fibers. It is easy to check that the particulate composite is a special case of the general relations (Eqs. (12a) and (13)). The influence of the fiber's shape is characterized by the coefficients $k_{3D}/3K_{3D}$ and $k_{3D}/5\mu_{3D}$.

2.3. Composites with aligned fibers

For the composite with aligned fibers, the composite as a whole is transverse isotropic. If we take the symmetric axis of the ellipsoidal fiber as$x_1$in a local coordinate system, and note $\boldsymbol{T}'=[\boldsymbol{I}+\boldsymbol{P}_1'(\boldsymbol{L}_1-\boldsymbol{L}_0)]^{-1}=(2k_T,l_T,l_T',n_T,2m_T,2p_T)$, the moduli of the composite, fiber and matrix are noted respectively by $\boldsymbol{L}_c=(2k_c,l_c,l_c,n_c,2m_c,2p_c)$, and $\boldsymbol{L}_i=(2k_i,l_i,l_i,n_i,2m_i,2p_i)(i=0,1)$, where $k_i=-K_i+\mu_i/3$, $l_i=K_i-2\mu_i/3$, $n_i=K_i+4\mu_i/3$, $m_i=p_i=\mu_i$. A fourth order tensor $\boldsymbol{Q}$, which is written as $\boldsymbol{Q}=(c,g,h,d,e,f)$, it can be shown that $\boldsymbol{Q}:\widetilde{\boldsymbol{I}}=\widetilde{\boldsymbol{Q}}$ is a second order tensor with non zero components $\widetilde{Q}_{11}=d+2g,\ \widetilde{Q}_{22}=\widetilde{Q}_{33}=h+c$. The nonzero components of the tensor $\boldsymbol{Q}\circ\widetilde{\boldsymbol{I}}=\widetilde{\boldsymbol{Q}}$ are $\widetilde{Q}_{11}=d+e,\ \widetilde{Q}_{22}=\widetilde{Q}_{33}=f+(c+e)/2$, and the nonzero components of the tensor $\widetilde{\boldsymbol{I}}:\boldsymbol{Q}=\widetilde{\boldsymbol{Q}}$ are $\widetilde{Q}_{11}=d+2h,\ \widetilde{Q}_{22}=\widetilde{Q}_{33}=g+c$.

If we note $[(\boldsymbol{L}_c-\boldsymbol{L}_0)^{-1}(\boldsymbol{L}_1-\boldsymbol{L}_0)-\boldsymbol{I}]=(2k_x,l_x,l_x,n_x,2m_x,2p_x)$, for the aligned fibers we have $\{\boldsymbol{T}_1\}=\boldsymbol{T}'_1$. So the following tensors can be expressed as:

$$(\boldsymbol{k}_c-\boldsymbol{k}_0)^{-1}(\boldsymbol{k}_1-\boldsymbol{k}_0)-\widetilde{\boldsymbol{I}}]=\bar{k}_{11}\boldsymbol{e}_1\otimes\boldsymbol{e}_1+\bar{k}_{22}(\boldsymbol{e}_2\otimes\boldsymbol{e}_2+\boldsymbol{e}_3\otimes\boldsymbol{e}_3) \tag{14}$$

$$\{\widetilde{\boldsymbol{T}}_1\}=\widetilde{\boldsymbol{T}}_1=\widetilde{T}_{11}\boldsymbol{e}_1\otimes\boldsymbol{e}_1+\widetilde{T}_{22}(\boldsymbol{e}_2\otimes\boldsymbol{e}_2+\boldsymbol{e}_3\otimes\boldsymbol{e}_3) \tag{15}$$

where $\widetilde{T}_{11},\widetilde{T}_{22}$ are given previously. $\bar{k}_{11},\bar{k}_{22}$ are related to the effective thermal conductivity of the composite, k_x, l_x, n_x, m_x, p_x are related to the effective engineering constants of the composite [17]. Especially, the axial direction Young's modulus, defined in [13], is expressed as $E_{c1}=n_x-l_x^2/k_x$. With the help of such notations, Eqs. (5a)–(5c) now become

$$2(2k_T+l'_T)l_x+(2l_T+n_T)n_x=\bar{k}_{11}\widetilde{T}_{11} \tag{16a}$$

$$2(2k_T+l'_T)k_x+(2l_T+n_T)l_x=\bar{k}_{22}\widetilde{T}_{22} \tag{16b}$$

$$2l'_Tl_x+n_Tn_x+4p_Tp_x=2\bar{k}_{11}\widetilde{T}_{11} \tag{16c}$$

$$2k_Tk_x+l_Tl_x+4m_Tm_x+2p_Tp_x=2\bar{k}_{22}\widetilde{T}_{22} \tag{16d}$$

$$4l'_Tk_x+n_Tn_x+2(l'_T+n_T)l_x=\bar{k}_{11}\widetilde{T}_{11} \tag{16e}$$

$$4k_Tk_x+l_Tn_x+2(l_T+k_T)l_x=\bar{k}_{22}\widetilde{T}_{22} \tag{16f}$$

It is easy to check that in the above six equations only five are independent, for example, it can be shown that 16(a) + 2 × 16(b) = 16(e) + 2 × 16(f). These five independent equations allow one to solve k_x,l_x,n_x,m_x,p_x in the term of the the variables $\bar{k}_{11},\bar{k}_{22}$, the cross-link between effective modulus and effective thermal conductivity can then be established. The detail expressions are complicated, and they will not be listed in this paper. It is checked that for an isotropic particulate composite, the results presented by Eqs. (7a) and (8) can be recovered.

2.4. Composites with planar randomly oriented fibers

In this situation, the composite as a whole is still transverse isotropic. If locally the symmetric axis is attached with x'_1 and the fibers are randomly oriented in x_1-x_2 plane, the composite is transversely isotropic with the symmetric axis x_3. We note $\boldsymbol{T}'=\left[\boldsymbol{I}+\boldsymbol{P}'_1(\boldsymbol{L}_1-\boldsymbol{L}_0)\right]^{-1}=\{2k_T,l_T,l'_T,n_T,2m_T,2p_T\}$, which is symmetric with respect to the axis x'_1 in the local coordinate system. The orientational average $\{\boldsymbol{T}_1\}$ of the tensor$\boldsymbol{T}_1$ is symmetric with respect to the axis x_3, and also the effective modulus of the composite. We still note $[(\boldsymbol{L}_c-\boldsymbol{L}_0)^{-1}(\boldsymbol{L}_1-\boldsymbol{L}_0)-\boldsymbol{I}]=(2k_x,l_x,l_x,n_x,2m_x,2p_x)$ and $\{\boldsymbol{T}_1\}=\left(2\bar{k}_T,\bar{l}_T,\bar{l}'_T,\bar{n}_T,2\bar{m}_T,2\bar{p}_T\right)$, the relation between $\boldsymbol{T}_1$ and $\{\boldsymbol{T}_1\}$ and the matrix form of a tensor with x_3 as symmetric axis are provided in the appendix. For thermal conductivity

$$[(\boldsymbol{k}_c-\boldsymbol{k}_0)^{-1}(\boldsymbol{k}_1-\boldsymbol{k}_0)-\widetilde{\boldsymbol{I}}]=\bar{k}_{11}(\boldsymbol{e}_1\otimes\boldsymbol{e}_1+\boldsymbol{e}_2\otimes\boldsymbol{e}_2)+\bar{k}_{33}\boldsymbol{e}_3\otimes\boldsymbol{e}_3 \tag{17}$$

$$\{\widetilde{\boldsymbol{T}}_1\}=\widehat{T}_{11}(\boldsymbol{e}_1\otimes\boldsymbol{e}_1+\boldsymbol{e}_2\otimes\boldsymbol{e}_2)+\widehat{T}_{33}\boldsymbol{e}_3\otimes\boldsymbol{e}_3) \tag{18}$$

where $\widehat{T}_{11}=\widehat{T}_{22}=\frac{1}{2}(\widetilde{T}_{11}+\widetilde{T}_{22})$, $\widehat{T}_{33}=\widetilde{T}_{22}$. $\bar{k}_{11},\bar{k}_{22}$ are related directly to the effective thermal conductivity of the composite, k_x,l_x,n_x,m_x,p_x are related to the effective engineering constants [17]. Eqs. (5a)–(5c) now become

$$2(2\bar{k}_T+\bar{l}_T)k_x+(2\bar{l}'_T+\bar{n}_T)l_x=\bar{k}_{11}\widehat{T}_{11} \tag{19a}$$

$$2(2\bar{k}_T+\bar{l}_T)l_x+(2\bar{l}'_T+\bar{n}_T)n_x=\bar{k}_{33}\widehat{T}_{33} \tag{19b}$$

$$2\bar{k}_Tk_x+l'_Tl_x+2\bar{m}_Tm_x+4\bar{p}_Tp_x=\bar{k}_{11}\widehat{T}_{11} \tag{19c}$$

$$2\bar{l}_Tl_x+4\bar{m}_Tm_x+\bar{n}_Tn_x=\bar{k}_{33}\widehat{T}_{33} \tag{19d}$$

$$4\bar{k}_Tk_x+l'_Tn_x+2(k_T+l'_T)l_x=\bar{k}_{11}\widehat{T}_{11} \tag{19e}$$

$$4\bar{l}_Tk_x+\bar{n}_Tn_x+2(l_T+n_T)l_x=\bar{k}_{33}\widehat{T}_{33} \tag{19f}$$

From Eq. (19), the cross-link relations of planar randomly oriented composites can then be derived. Detailed expressions will not be listed in this paper. It is easy to show that be in above six equations, only five are independent. In the following, the established analytical cross-link relation will be checked by finite element simulation, they will also be compared with experiment in the literature.

3. Numerical simulation and application

The above explicit cross-link relations have been established by an approximate micromechanical method, namely Mori–Tanaka's mean field theory. In order to check whether cross-link relations are sensitive to specified microstructure of composite, we will in this section numerically generate some fiber composites with specific microstructures, and compute the corresponding cross-link relations. The numerically obtained cross-link relations will be compared with those obtained previously by Mori–Tanaka method. They will also be compared with the experimental results given by Rousion et al. [13].

Three types of composites are generated: aligned ellipsoidal fibers, planar randomly oriented fibers and space randomly oriented fibers. Three aspect ratios of the fiber, namely, 1:100, 1:10 and 1:1 are examined for each case. For each type of the microstructure, different volume fractions of the fiber are analyzed. The typical microstructures generated for different types of composites are shown in Figs. 1–4. In the realization of microstructure, non-overlap for fibers is guaranteed. Moreover, periodic boundary conditions are considered here: when a phase point of fiber appears outside the digital image, it is periodically continued on the other side of the given system. In FEM simulations, every image is considered as a representative volume element (RVE) for the corre-

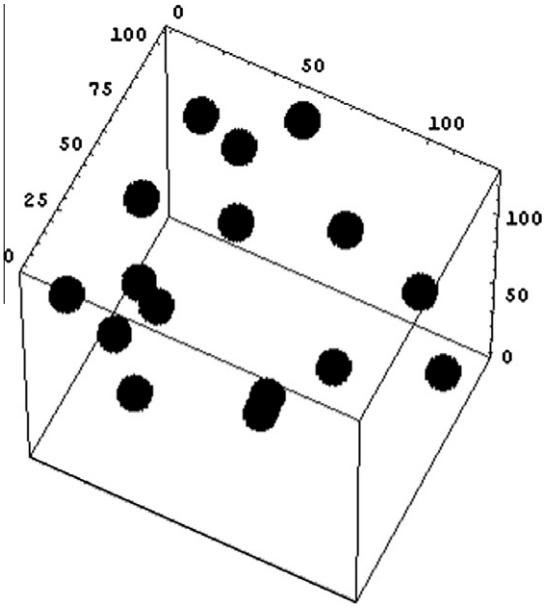

Fig. 1. Microstructures generated with impenetrate spheres (particulate composite).

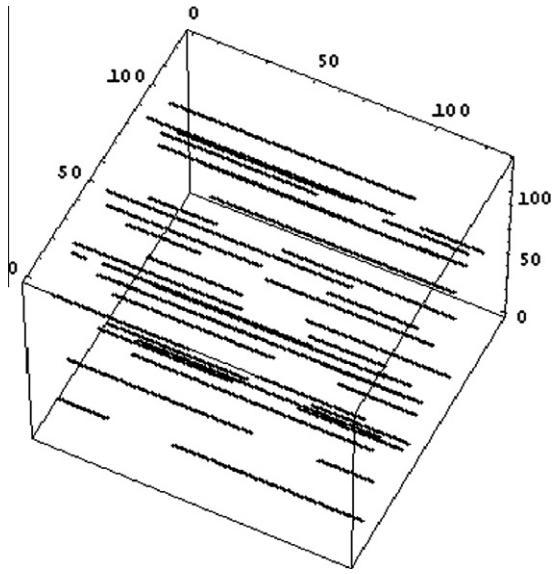

Fig. 2. Microstructures generated with aligned fibers along x_1 (aspect ratio = 1:100).

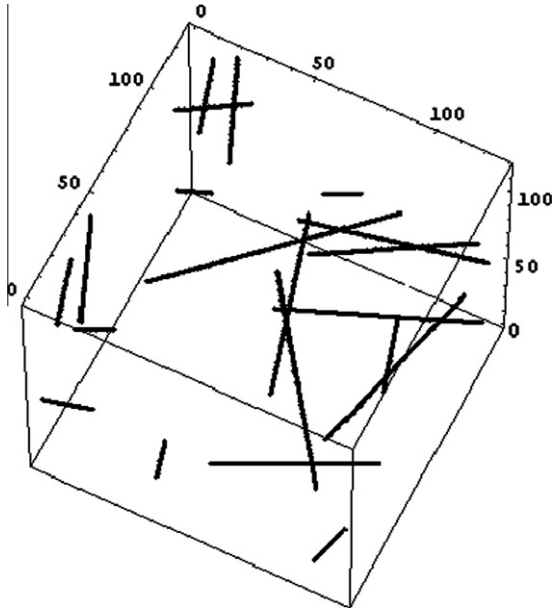

Fig. 3. Microstructures generated with planar randomly oriented fibers (in $x_1 - x_2$ plane)(aspect ratio = 1:100).

sponding composite. The digital-image-based finite element method developed by Garboczi [18] is utilized for computing the effective property of the composite. The accuracy of this method was discussed by Garboczi and Day [19], they found that a cube of $128 \times 128 \times 128$ pixels can provide a good accuracy. This is also checked for fiber composite. In the following simulation, the digital images need to be firstly saved in an ASCII format representing the cubic pixels value of different phases, FE program developed by Garboczi [18] is used for computing the local field. In the computation, each pixel is considered to be an element in FE formulations. Unit three-axial macroscopic strains are properly imposed on the boundary of the RVE, and local stresses as well as their spatial averages over the RVE are evaluated, and these average stress and strain will be employed to compute the effective modulus of the composite. The detail exposition of the method can be found

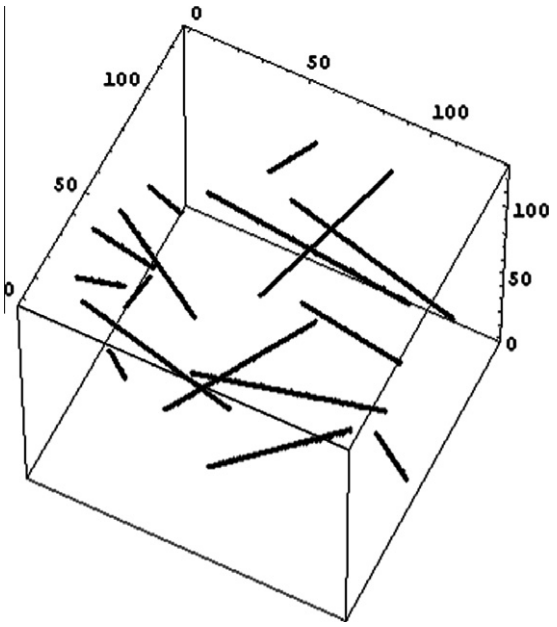

Fig. 4. Microstructures generated with space randomly oriented fibers (aspect ratio = 1:100).

Table 1
Material constants of the composite used in the numerical study.

	Matrix	Fiber
Young's modulus E (GPa) [13]	3.2	71
Poisson's ratio v	0.4	0.22
Thermal conductivity k (W/m C) [13]	0.2	1.04

in the reference [18]. In a similar way, for the effective thermal conductivity, a constant gradient of temperature is imposed on the boundary: as a result, the local heat flux is calculated, and then averaged over the RVE, which gives the effective thermal conductivity for the same composite. The numerical cross-link between the effective modulus and thermal conductivity of the composite can then be established.

In order to evaluate the accuracy for the obtained cross-link relation, the analytical and numerical results are further compared with the experimental results conducted by Rousion et al. [13]. The material constants used in the numerical study can be found in Table 1 for the matrix and fiber of the composite, respectively. In their experiment [13], only the composites with aligned fibers and planar randomly oriented fibers are examined. The aspect ratio of the fiber in the experiment can be considered to be infinite, however in our numerical simulation, we take the aspect ratio 100 to simulate the long fiber.

For the composite with aligned fibers, the comparison results are shown in Fig. 5 for the effective modulus and conductivity along the direction of fiber. In the figure, E_{c1} and k_{c1} represent, respectively, the effective Young's modulus and thermal conductivity of the composite in the axial direction as defined in [13]. It is found that the analytical cross-link relation agrees well with numerical ones obtained by FE analysis for different aspect ratios and volume concentration of fibers. Both analytical and numerical cross-link relations are in a good agreement with the experiment conducted by Rousion et al. [13].

The cross-link relations for composite with planar randomly oriented fibers are illustrated in Fig. 6 for different methods. In the figure, E_{c1} and k_{c1} represent the effective Young's modulus and thermal conductivity of the composite in the axial direction as defined in [13], respectively. The results show that there is an

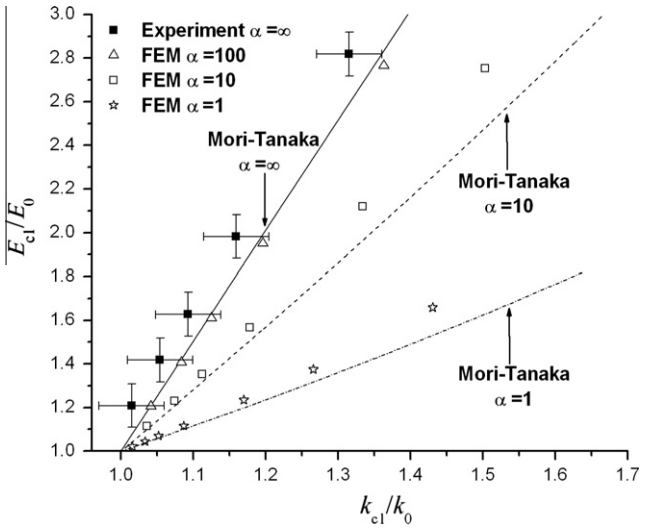

Fig. 5. Cross-link relations for composites with aligned fibers for different methods and aspect ratios (E_0:E_1 = 1:22).

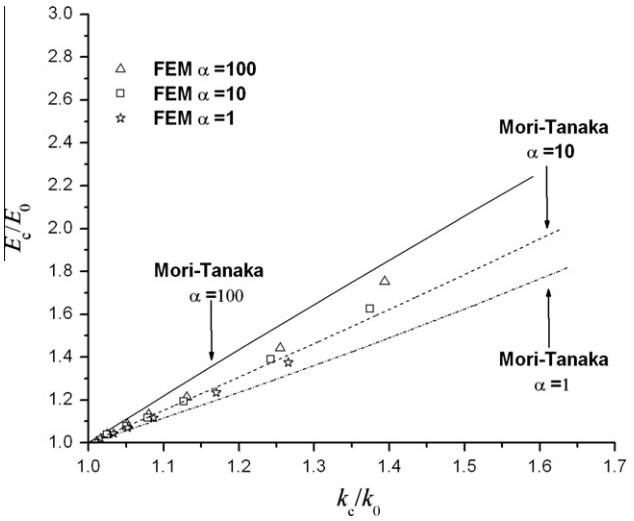

Fig. 7. Cross-link relations for composites with space randomly oriented fibers for different methods and aspect ratios (E_0:E_1 = 1:22).

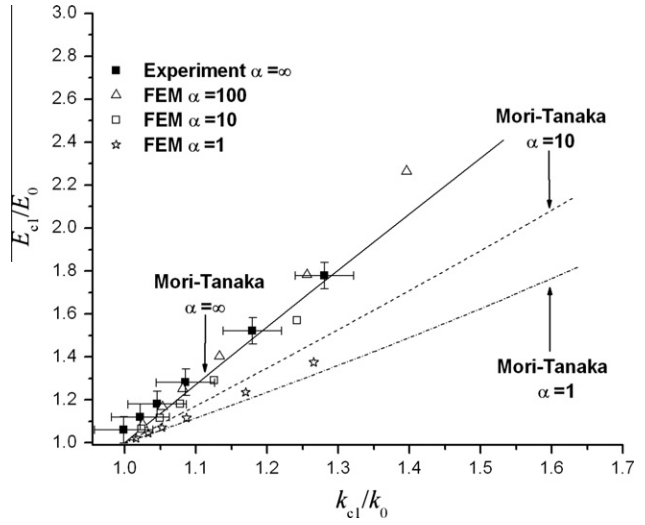

Fig. 6. Cross-link relations for composites with planar randomly oriented fibers for different methods and aspect ratios (E_0:E_1 = 1:22).

excellent agreement between analytical and numerical cross-link relations for different aspect ratios and volume concentration of the fibers. They are also in a reasonable agreement, and the discrepancy may be attributed to complexity of microstructure in the experiment.

Fig. 7 gives the comparison results for a composite with space randomly oriented fibers, where the composite is isotropic with the effective Young's modulus and thermal conductivity E_c and k_c. Since there is no experimental result, we present only the results obtained by analytical and numerical methods. It is found that the numerical cross-link relation is insensitive to the shape of the fiber for the composite with space randomly oriented fibers, which agrees with the observation of Kachanov et al. [5] and Zhao et al. [7] that the cross-link of a two-phase composite is relatively insensitive to the exact phase shape distribution; however the analytically obtained cross-link relation shows weak dependence on the fiber's shape. The discrepancy is expected because of the approximation of the Mori–Tanaka method, especially for the composite with high modulus contrast and high volume concentrations of fibers [8,15]. The corresponding effective properties may vary dramatically near the percolation threshold.

In view of results for different microstructures in Figs. 5–7, the obtained cross-link relations can be found to become less and less sensitive to the fiber's shape, when materials go from composites with aligned fibers, composites with planar randomly oriented fibers, to composites with space randomly oriented fibers. Most noticeably, such decreasing dependence of the fiber's shape with the decrease of the material anisotropy has been captured by both the analytical and numerical predictions of cross-link relations in the study.

4. Conclusions

Explicit cross-link relations between effective elastic modulus and thermal conductivity for composites with different fiber orientation are established by an approximate Mori–Tanaka micromechanical method. These cross-link relations are also compared with those obtained through finite element method. A good correlation is observed between analytical and numerical cross-link relations for the composite with aligned fibers and planar randomly oriented fibers, and they both agree well with the experiment results available in the literature. In addition, it needs to be mentioned that the sensitivity of cross-link relations to the fiber's shape depends on the extent of anisotropic behavior of composites, as predicted by both analytical and numerical methods.

Acknowledgment

This work was supported by the National Natural Science Foundation of China through Grant 10325210 and 11072031.

Appendix A

For an ellipsoidal fiber with x_3 as the symmetric axis, the aspect ratio of the ellipsoid is denoted byρ, the nonzero components of the tensors $\boldsymbol{P}, \widetilde{\boldsymbol{P}}$ are respectively

$$\widetilde{P}_{11} = \frac{1}{k_0}(1-g),\ \widetilde{P}_{22} = \widetilde{P}_{33} = \frac{1}{2k_0}g$$

And

$$P_{1111} = \frac{1}{2G_0(1-v_0)}\left[(1-2v_0)+\frac{\rho^2}{\rho^2-1}\right] + \frac{1}{4G_0(1-v_0)}\left[4(v_0-1)-\frac{3}{\rho^2-1}\right]g$$

$$P_{2222} = P_{3333} = \frac{3}{16G_0(1-v_0)}\frac{\rho^2}{\rho^2-1}+\frac{1}{32G_0(1-v_0)}\left[4(1-4v_0)-\frac{9}{\rho^2-1}\right]g$$

$$P_{1212} = P_{1313} = -\frac{1}{4G_0(1-v_0)}\left[v_0+\frac{1}{\rho^2-1}\right] + \frac{1}{8G_0(1-v_0)}\left[(1+v_0)+\frac{3}{\rho^2-1}\right]g$$

$$P_{2323} = \frac{1}{16G_0(1-v_0)}\frac{\rho^2}{\rho^2-1}+\frac{1}{32G_0(1-v_0)}\left[4(1-2v_0)-\frac{3}{\rho^2-1}\right]g$$

$$P_{1122} = P_{1133} = P_{2211} = P_{3311} = -\frac{1}{4G_0(1-v_0)}\frac{\rho^2}{\rho^2-1}+\frac{1}{8G_0(1-v_0)}\left[\frac{1+2\rho^2}{\rho^2-1}\right]g$$

$$P_{2233} = P_{3322} = \frac{1}{16G_0(1-v_0)}\frac{\rho^2}{\rho^2-1}+\frac{1}{32G_0(1-v_0)}\left[\frac{1-4\rho^2}{\rho^2-1}\right]g$$

when $\rho > 1$

$$g = \frac{\rho}{(\rho^2-1)^{3/2}}\left[\rho\sqrt{(\rho^2-1)}-\arccos h(\rho)\right]$$

And when $\rho < 1$

$$g = \frac{\rho}{(1-\rho^2)^{3/2}}\left[\arccos(\rho)-\rho\sqrt{(1-\rho^2)}\right]$$

References

[1] J.R. Bristow, Brit. J. Appl. Phys. 11 (1960) 81–85.
[2] V.M. Levin, Mech. Solids 2 (1967) 58–61.
[3] T.J. Lu, C.G. Levi, H.N.G. Wadley, A.G. Evans, J. Am. Ceram. Soc. 84 (2001) 2937–2946.
[4] I. Sevostianov, M. Kachanov, Mater. Sci. Eng. A 297 (2001) 235–343.
[5] M. Kachanov, I. Sevostianov, B. Shafiro, J. Mech. Phys. Solids 49 (2001) 1–25.
[6] I. Sevostianov, M. Kachanov, J. Mech. Phys. Solids 50 (2002) 253–282.
[7] H.F. Zhao, G.K. Hu, T.J. Lu, Int. J. Fracture 126 (2004) L11–L18.
[8] H.F. Zhao, G.K. Hu, T.J. Lu, Comput. Mater. Sci. 35 (2006) 408–415.
[9] I. Sevostianov, M. Kachanov, Adv. Appl. Mech. 42 (2009) 69–252.
[10] I. Sevostianov, M. Kachanov, Int. J. Eng. Sci. 48 (2010) 1702–1708.
[11] I. Sevostianov, J. Kovaik, F. Simanik, Int. J. Fracture 144 (2002) L23–L28.
[12] I. Sevostianov, M. Kachanov, Mater. Sci. Eng. A 360 (2003) 339–344.
[13] D. Rousion, M. Varejka, J. Picot, Can. J. Chem. Eng. 80 (2002) 943–947.
[14] T. Mori, K. Tanaka, Acta. Metall. Mater. 21 (1973) 571–574.
[15] G.K. Hu, G.J. Weng, Acta Mech. 140 (2000) 31–40.
[16] Z. Hashin, J. Appl. Mech. 50 (1983) 481–505.
[17] G.L. Shen, G.K. Hu, Mechanics of Composite Materials, Tsinghua University Press & Springer Press, Beijing, 2006.
[18] E.J. Garboczi, NIST Internal Report 6269, 1998.
[19] E.J. Garboczi, A.J. Day, J. Mech. Phys. Solids 43 (1995) 1349–1362.